SELECTIVE ADSORPTION / ABSORPTION OF FORMAMIDE IN NACL CRYSTALS GROWING FROM SOLUTION

Cover Page

SELECTIVE ADSORPTION / ABSORPTION OF FORMAMIDE IN NACL CRYSTALS GROWING FROM SOLUTION

Linda Pastero[1], Dino Aquilano[1], Massimo Moret[2]*

[1]Dipartimento di Scienze della Terra, Università degli Studi di Torino - Via Valperga Caluso 35 - I 10125 Torino

[2]Dipartimento di Scienza dei Materiali, Università degli Studi di Milano Bicocca - Via Roberto Cozzi 53 - I 20125 Milano

CONTACT DETAILS:

dino.aquilano@unito.it

Tel: +39116705125

Fax: +39116705128

Title Page

Selective adsorption / absorption of formamide in NaCl crystals growing from solution

Linda Pastero[1], Dino Aquilano[1], Massimo Moret[2]*

[1]Dipartimento di Scienze della Terra, Università degli Studi di Torino - Via Valperga Caluso 35 - I 10125 Torino

[2]Dipartimento di Scienza dei Materiali, Università degli Studi di Milano Bicocca - Via Roberto Cozzi 53 - I 20125 Milano

AUTHOR EMAIL ADDRESS : dino.aquilano@unito.it

RECEIVED DATE (to be automatically inserted after your manuscript is accepted if required according to the journal that you are submitting your paper to)

TITLE RUNNING HEAD Selective ad / ab-sorption of formamide in NaCl crystals

CORRESPONDING AUTHOR FOOTNOTE E-mail:dino.aquilano@unito.it Tel: +390116705125 Fax: +390116705128

ABSTRACT

NaCl crystals were obtained from water-formamide (H-CO-NH_2) solutions, either by slow evaporation at 30 °C or by programmed cooling of solutions saturated at 95°C, the formamide concentration ranging from 0 to 100% (in weight). Accordingly, the crystal morphology changes from {100} (pure aqueous solution) to {100} + {111} (water-formamide solutions) to {111} (pure formamide solution). X-ray powder diffraction diagrams, carried out on the bulky crystallized population, prove that formamide is not only adsorbed on the $\{111\}_{NaCl}$ octahedron but is also selectively captured within the {111} growth sectors. The excellent 2D-lattice coincidences between the d_{101} layers of formamide and the NaCl - d_{111} ones suggest that formamide can be adsorbed in the form of ordered epitaxial layers; further, the striking equivalence between the thickness of the elementary layers d_{111}^{NaCl} and $d_{101}^{formamide}$ indicates that formamide is allowed to be buried (absorption) in the growing crystal. Moreover, empirical force field calculations carried out on reconstructed {111} NaCl surfaces, both Na^+ and Cl^- terminated, allowed to evaluate the adhesion energy between the formamide epitaxial layers and the underlying $\{111\}_{NaCl}$ substrate. Hence, one can definitively state that formamide is not only an habit modifier of NaCl crystals, but that "anomalous NaCl / formamide mixed crystals" form, limited to the {111} NaCl growth sectors.

KEYWORDS Sodium chloride, formamide, adsorption, absorption, crystal growth, anomalous mixed crystals, 2D epitaxy

1. Introduction

Recently, it was demonstrated that the bulk structure of calcite crystals, grown in aqueous solution and in the presence of lithium, reveals an intimate interaction between the structures of $CaCO_3$ (mineral calcite) and Li_2CO_3 (mineral zabuyelite), even if the concentration of lithium in solution is largely lower than that needed to precipitate 3D- zabuyelite crystals[1]. As a matter of fact, it was shown that lithium is not randomly absorbed into the lattice of calcite during growth and that an "anomalous $CaCO_3/Li_2CO_3$ mixed crystal", in the sense of Gaubert[2], Seifert[3], Johnsen[4], Neuhaus[5] and Hartman[6] can form, limited to the growth sectors of $\{0001\}$ and $\{10\bar{1}4\}$ forms of calcite. Moreover, we proved that when lithium concentration is continuously increased in the mother phase, lithium is not only ad-sorbed through one-dimensional (1D) and/or two-dimensional (2D) epitaxies on the just mentioned forms of calcite but is selectively absorbed in the $\{0001\}$ and $\{10\bar{1}4\}$ growth sectors as well[7]. According to the definition of anomalous mixed crystal, this means that the lattice coincidences should not be limited to the 2D lattices ruling the calcite/zabuyelite epitaxial interfaces but that also the thicknesses of the facing interfacial layers show a negligible misfit. In other words, the parametric coincidence in the three space directions, between the adsorbing and the absorbing crystal phases, are largely fulfilled and then an anomalous mixed crystal can be formed.

Furthermore, the foreign adsorption resulting in 2D-epitaxy has been very recently invoked when explaining the enantiospecificity of the adsorption of the L-Aspartic acid onto the $\{21\bar{3}4\}$ scalenohedron form of calcite[8]. In this case, it was crucial to acknowledge that the observed enantiospecificity cannot be explained by the random molecular adsorption but that only the cooperative molecular approach (intrinsic to the 2D epitaxy) leads to the correct way of interpretation. Starting from these results and persuaded that the significant morphological crystal modifications occurring in the presence of foreign adsorption cannot be due to the only action of isolated adsorbed units (atoms, ions or molecules), we returned to the $\{100\} \rightarrow \{111\}$ habit change occurring in NaCl crystals growing from

aqueous solutions in the presence of formamide (H-CO-NH_2)[9,10]. This is a long debated case study; nevertheless a univocal interpretation of the experimental data has not been given up to now.

Concerning the reasons why it is interesting to investigate the effects of additives (foreign ions and molecules) on the NaCl crystal morphology, it is worth remembering that these effects have been known since the earliest example of the {100}→{100}+{111} NaCl change induced by urea[11]. Usually, additives act in two main ways: (i) as crystallization inhibitors, preventing or delaying the formation of stable nuclei, although in some cases they can work as nucleation promoters; (ii) as habit modifiers, by adsorption onto specific faces of a growing crystal, thus decreasing (or increasing) their growth rates. Significant overviews have been published on this general and fundamental topic[12]. Regarding the NaCl crystal, we remember a sound example of the inhibiting effects of a specific additive (the ferrocyanide ion) on NaCl crystallization. The anion $Fe(CN)_6^{4-}$ is commonly used, in low concentrations, to prevent or control the NaCl nucleation and growth in weathered rocks and construction materials (e.g., stones and concrete)[13], and to avoid salt crystallization damage due to NaCl sub-florescence growth in porous stones[14]. Alternatively it is used as an anti-caking agent for road de-icing [15] or as an additive for the food industry [16]. Formamide is not known for its efficiency as NaCl habit modifier at very low or low concentrations or for its industrial applications. Nevertheless, its ability to progressively modify the NaCl habit (from pure cube to pure octahedron)[9,10] when its concentration in aqueous solutions varies from 0 to 100%, makes of relevant interest to investigate, from the fundamental point of view, the growth mechanisms in the system: formamide-water- NaCl crystal.

2. {100} → {111} habit change in NaCl crystals growing from aqueous solutions in the presence of formamide. The literature data.

The early work on this topic dates back to Gille and Spangenberg[9] who found the {100} → {111} habit change in NaCl crystals obtained from evaporating aqueous solutions in the presence of formamide, as represented in Figure 1. Much later, Bienfait et al.[10] identified the stability domains of the cube and the

octahedron (morphodrome) as a function of two parameters: the initial supersaturation of the solution with respect to NaCl and the formamide concentration in solution (see Figure 2). It is known, since the papers by the Kern's group on this topics, that formamide exerts on NaCl crystals an influence similar to that obtained with urea[17], that is, formamide lowers the critical supersaturation value (β_{cr}), at which the transition {100}→{111} occurs, with respect to that measured in pure water solution. In fact, the {100}→{111} transition was observed at $\beta_{cr} = 1.004$ in pure formamide, while the corresponding value, in pure water, reaches $\beta_{cr} = 1.23$. This was interpreted by considering that both urea and formamide have a similar steric hindrance that allows them to occupy the vacant sites, on the octopolar reconstructed {111} form, where the surface electric field reaches its highest value. The stability of the {111} form should further increase (with respect to that obtained in pure aqueous solution) since the dipole moment of urea and formamide is definitely higher than that of the water molecule.

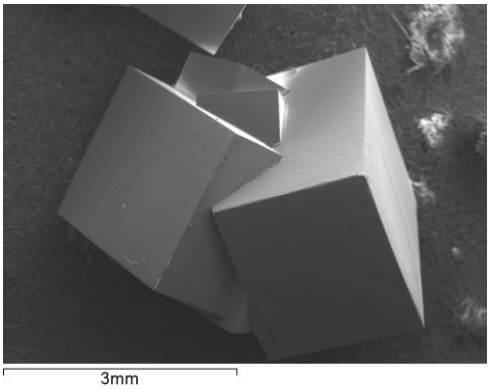

a)

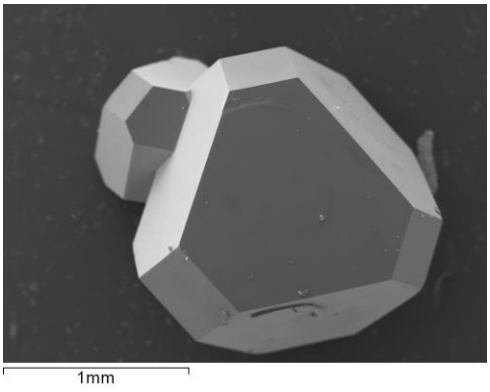

b)

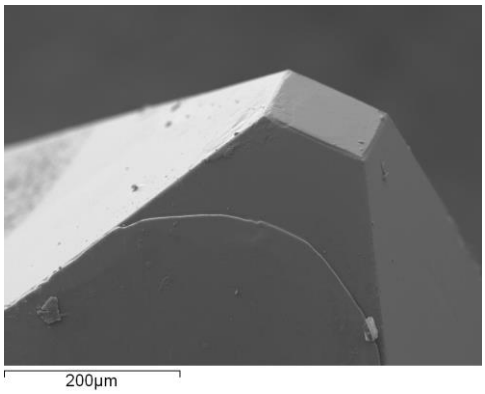

c)

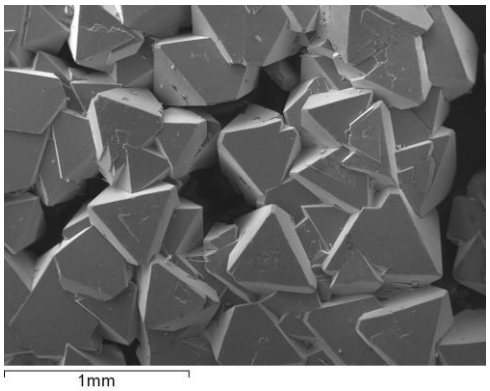

d)

Figure 1. SEM pictures of NaCl crystals we grew from solution by evaporation at 25°C. a) {100} form, from pure aqueous solution; b) {100}+{111} forms, from solution containing 20%, in weight, of formamide; c) a macrostep spreading on the {111} form showing the layer growth of the octahedron in the presence of formamide (detail of the preceding case); d) uniqueness of the {111} form, grown from pure formamide solution.

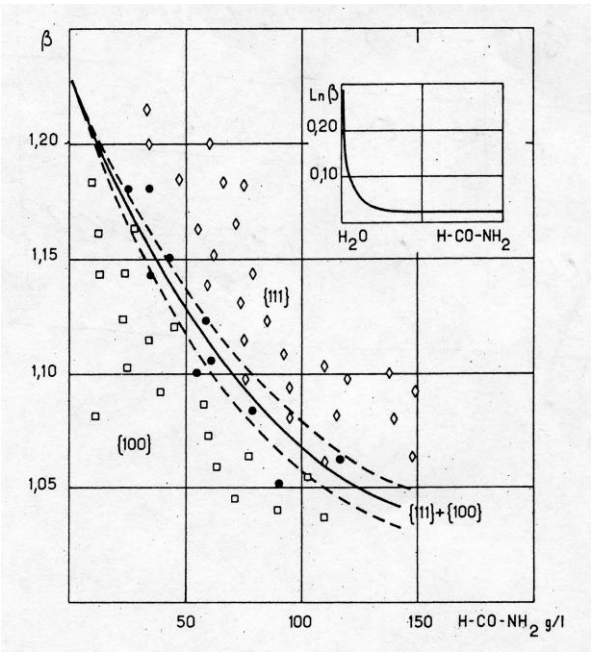

Figure 2. Morphodrome of NaCl crystals grown from aqueous solutions in the presence of formamide (concentrations, in g/L, on the *x*-axis); on the *y*-axis, the initial supersaturation of the solution with respect to NaCl. In the inset: the morphodrome represents the situation comprised between the limiting cases of pure water and pure formamide solutions. Reprinted with permission from ref 10. Copyright 1965 Centre National de la Recherche Scientifique

Recently, Radenovič et al.[18-24] confirmed the just mentioned observations by evaporating at room temperature NaCl aqueous solutions containing up to 30% of formamide, and outlined that the presence of formamide enhances the quality of NaCl crystals, since the number of fluid inclusions sharply decreases with respect to those found after growth from pure aqueous solutions. Moreover, through a surface X-ray diffraction (SXRD) determination of the {111} NaCl-liquid interface structure and using

ultra-thin water or formamide adsorbed liquid layers, they ascertained that the crystal surface is smooth at an atomic level and is not reconstructed. This revealed small differences in surface structure between the water or formamide liquid layers, that nevertheless lead to dramatic differences in crystal morphology. From SXRD, they determined as well that the {111} surface is Na^+ terminated for both environmental conditions and that 0.25–0.5 of a monolayer of laterally disordered Cl^- ions is located on top of a fully ordered Na^+ crystal surface with occupancy 0.75–1.0. Hence, they concluded that the polar surface is stabilized through the formation of an electrochemical double layer.

A further consideration has been proposed by the Vlieg's group to detail the influence of formamide on the NaCl morphological change: they noticed that for alkali halide crystals grown from saturated formamide solutions, the appearance of the {111} form is strictly related to unit cell size. Octahedrons appear starting from NaF crystals (unit cell size = 4.62 Å) to KCl with a unit cell of 6.28 Å. Thus, they concluded that all alkali halide crystals with dimensions outside this range of unit cells crystallize as cubes and this confirmed that, apart from dipole-ion interaction, also the volume and the shape of the molecules are important for the stabilization of the {111} alkali halide surfaces by adsorption.

Suspecting that such a dramatic change of morphology may be hardly interpreted in the light of the sole interactions between isolated molecules and the crystal surface, we investigated the structure of formamide in order to find if any cooperative effect (such as an epitaxial relationships) can set up between the crystal structures of NaCl (host phase) and formamide (guest phase). To do this, we started from the structure of formamide.

3. The structure of formamide

According to the structure determinations[23-25], the monoclinic (S.G. $P2_1/n$) formamide crystals can be viewed as puckered sheets of molecules; adjacent sheets, which are parallel to the 101 plane, are separated by the equidistance d_{101} reaching the value of 3.09 Å, at 0°C, just below the melting point at room pressure (see Table 1). Within the sheets, pairs of molecules associate around centers of symmetry to form almost coplanar bimolecular units. Puckering of the sheets results from the tilt of the bimolecular units relative to one another. N-H···O bonds of two types cross-link the chains forming each

sheet: the α (H-bonds), 2.93 Å long, link monomers to form bimolecular units, while the β (H-bonds), 2.88 Å long, link bimolecular units together. In the light of the Hartman-Perdok theory, we found two periodic bond chains (PBCs hereinafter) running within the d_{101} formamide layers: the PBC [010] developing along the screw A_2 axis through α (H-bonds) and the PBC $[11\bar{1}]$ made by β (H-bonds). Looking at the formamide structure and remembering that no H-bonds can be found outside the d_{101} layers, it is easy to consider the {101} pinacoid as the most important F form of the crystal. Then, the theoretical crystal habit (at least from vapor phase) should be {101} platy. This is the main reason why we choose the 101 plane as the best candidate for a hypothetical epitaxy between a 2D layer of formamide and the growing NaCl -{111} form.

	Host crystal form: NaCl {111}	Guest crystal form: formamide {101}	misfit %	obliquity
2D-cell vectors (Å)	$[11\bar{2}] = 13.81$ $[1\dot{1}\,0] = 7.976$	$3/2[010] = 13.849$ $[10\dot{1}] = 8.167$	+ 0.282 +2.394	0°
Layer thickness (Å)	$d_{111} = 3.25$	$d_{101} = 3.095$	– 4.769	-----

Table 1. Lattice coincidences at the $\{111\}_{NaCl}/\{101\}_{formamide}$ interface. The formamide data are obtained from the extrapolation at T = 273 K, starting from three structures obtained at 223[23], 108[24] and 90 K[25], respectively.

From Table 1 one can be aware of a striking 2D-lattice coincidence that may set up both at the $\{111\}_{NaCl}/\{101\}_{formamide}$ interface and between the thickness of the elementary layers d_{111}^{NaCl} and $d_{101}^{formamide}$. All that means that it is worth searching for prove the existence of NaCl/formamide anomalous mixed crystals.

4. The {100} → {111} morphological change of NaCl due to formamide ad-sorption and its selective capture (absorption) in the bulk of the NaCl lattice

4.1. The experimental evidences from PXRD diagrams .

Starting from the experience acquired about the calcite/zabuyelite anomalous mixed crystals, we did not confine our attention to the morphology of the NaCl crystals grown in the presence of formamide, but investigated also their bulk structure, in order to find if the adsorption → absorption mechanism would also occur in this new case. Fig.3.1 shows the PXRD patterns (Cu-K$\alpha_{1,2}$), recorded at a temperature (T_{meas}), on different populations of NaCl crystals obtained at different crystallization temperature (T_c) and from solutions saturated at a temperature T_s and containing different concentrations of formamide (C_f, expressed in weight %). Two main (2θ) intervals, corresponding to the d_{111} and d_{002} spacing of the NaCl crystal are worthy of consideration:

- the first (2θ) interval: 27°≤ 2θ ≤ 28° related to the 111_{NaCl} plus the $101_{formamide}$ reflection (if any)
- the second (2θ) interval: 31°≤ 2θ ≤ 32.5° → related to the 002_{NaCl} reflection

4.1.1. The first (2θ) interval

$i_{(111)}$ - A saturated (T_s=95°C) NaCl aqueous solution (C_f =20%) was cooled down to −5°C, under a gradient of 20°/h. PXRD spectra were carried out at T= −5°C as well, on a large population of as grown {111} platy shaped and un-grinded crystals. Fig.3a, left side, shows two diffraction peaks. The first one, at lower 2θ values, corresponds to the $\lambda_{K\alpha 1}$ contribution of the reflection d_{111}^{NaCl}=3.258 Å. The second one, that is, the low intensity peak at 2θ =27.671, *cannot be indexed as a NaCl reflection* but as the $d_{101}^{formamide}$ = 3.221 Å (using the $\lambda_{K\alpha 1}$=1.54060 Å). This $d_{101}^{formamide}$ value is slightly higher (+4.07%) than the calculated one (3.095 Å) by extrapolation of structural data of the pure formamide. This means that NaCl crystals were able to capture formamide in their bulk during growth (either through fluid

inclusions or by absorption of ordered d_{101} layers, or both). In that case, to remove the ambiguity arising from the fact that the just mentioned patterns were obtained at T = –5°C where formamide is necessarily crystallized, other measurements have been made at T ≥ 2°C, that is, beyond its melting point. Therefore, all the experiments described in the following were performed by evaporating a solution (T_{ev}=30°C) and the corresponding PXRD patterns were carried out at T= 25°C.

$ii_{(111)}$ - NaCl crystals were formed from an evaporated water/formamide solution(C_f =20%). Their morphology is now made by dominating {100} and small {111} forms. The 111_{NaCl} peak is weakly

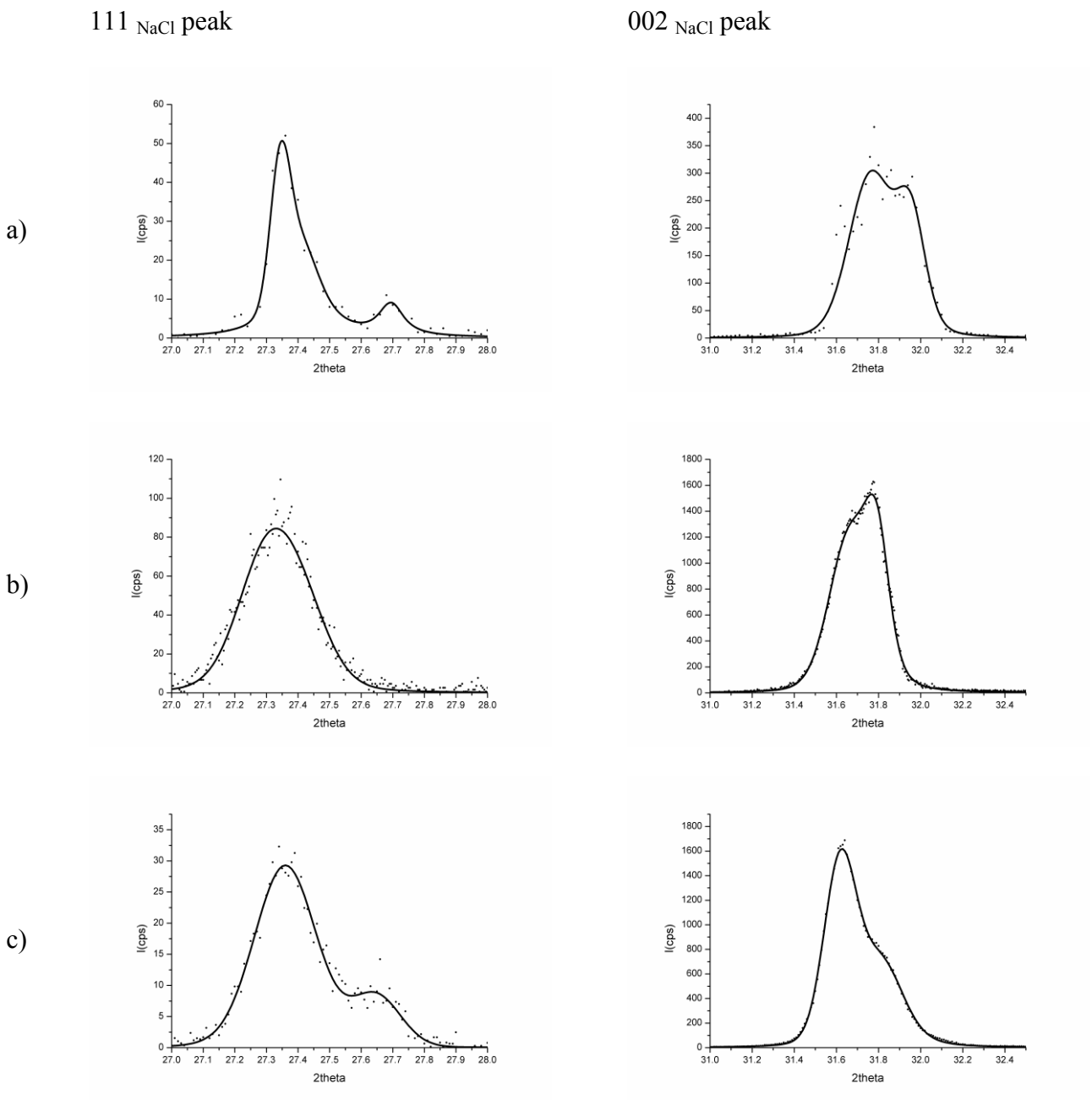

111 $_{NaCl}$ peak

002 $_{NaCl}$ peak

d)

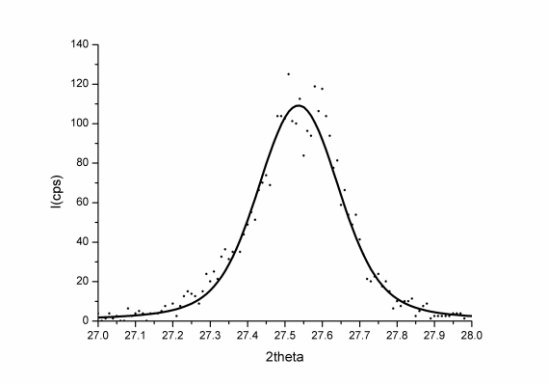

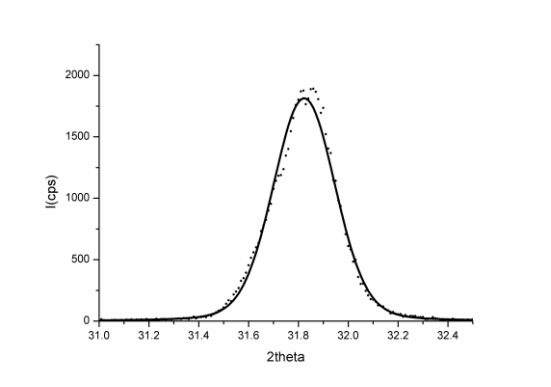

e)

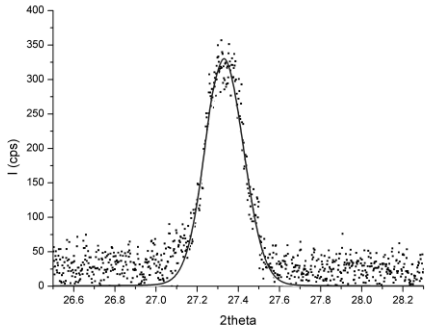

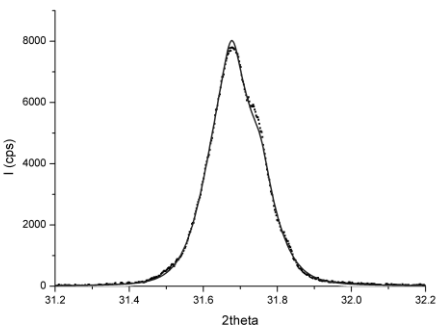

f)

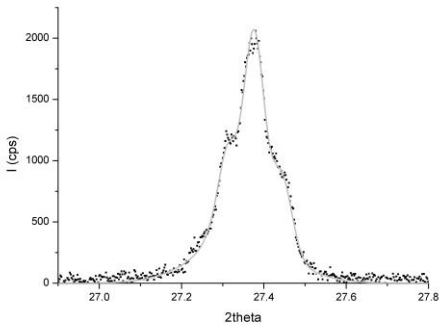

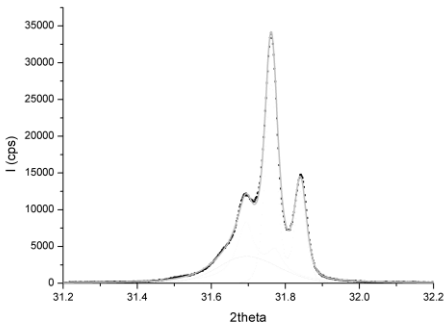

g)

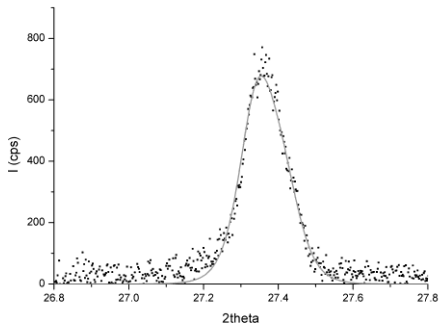

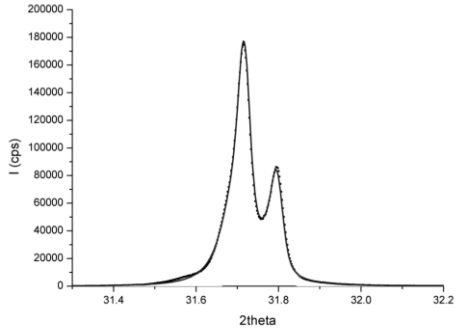

Figure 3. PXRD diagrams of NaCl crystals grown in the presence of variable concentrations (C_f, weight %) of formamide. (a) C_f =20; T_s= 95°C; T_c = -5°C; T_{meas} = -5°C. (b) C_f =20; T_s= 95°C; T_c = 30°C; T_{meas} = 25°C. (c) C_f =60; T_s= 95°C; T_c = 30°C; T_{meas} = 25°C. (d) C_f =100; T_s= 95°C; T_c = 30°C; T_{meas} = 25°C. (e) C_f = 0; T_s= 95°C; T_c = -10°C; T_{meas} = 25°C. (f) C_f =60; T_s= 95°C; T_c = -10°C; T_{meas} = 25°C; (g) C_f =100; T_s= 95°C; T_c = -10°C; T_{meas} = 25°C.

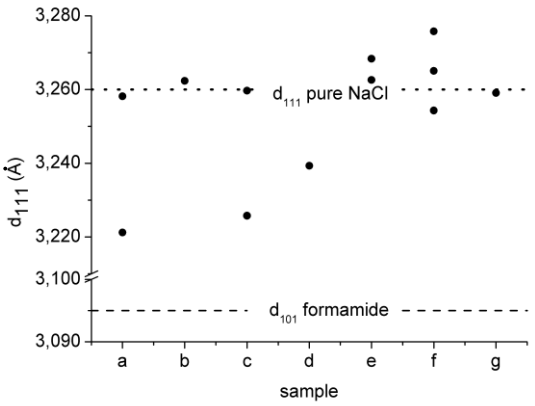

a)

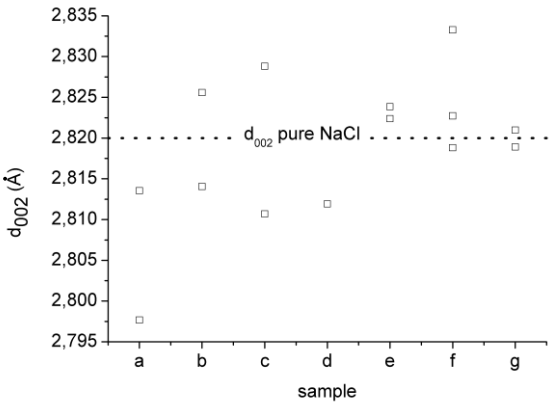

b)

Figure 4. Lattice spacing calculated from the decomposition of the diffraction peaks drawn in Fig.3**. (**a) d_{111} spacing from samples (a-g) compared with d_{111} from pure NaCl crystal (dotted line) and d_{101} from pure formamide (dashed line) ; (b) d_{002} spacing from samples (a-g) compared with d_{002} from pure NaCl crystal (dotted line).

asymmetric (due to the $\lambda_{K\alpha 1}$ component) and yields d_{111}^{NaCl}=3.262 Å. No other peak occurs in the observed 2θ range. (Fig.3b, left side) The small increase (+0.061%) of the d_{111}^{NaCl} value is not surprising, owing to the increased temperature of measurement (from –5 to +25°C). However, no adsorbed $d_{101}^{formamide}$ layers are found to be orderly absorbed in the growing NaCl crystal.

iii$_{(111)}$ - NaCl crystals were obtained from a new water/formamide solution (C_f =60%). Their morphology is now made by dominating {111} and small {100} forms. The full width at half maximum

(fwhm) of the 111_{NaCl} peak (d_{111}^{NaCl}=3.260 Å) increases with respect to the preceding case. A satellite peak occurs at 2θ =27.631 and corresponds to $d_{101}^{formamide}$ = 3.226 Å (Fig.3c, left side). Any effect of crystallization of formamide fluid inclusions must be excluded since both the crystallization and recording temperatures were largely higher than the melting point of formamide. Then, when the concentration of formamide competes with that of water, the $d_{101}^{formamide}$ layers are not only epitaxially adsorbed on the {111} NaCl surfaces but also buried in the growing crystal.

iv$_{(111)}$ - The just mentioned conclusion is spectacularly confirmed by NaCl crystals obtained from pure formamide solution. The only form is the {111} octahedron. XRPD patterns yielded a unique and symmetric peak which is located in between the 111_{NaCl} and the $101_{formamide}$ peaks.(Fig. 3d, left side) Thus, as a first approximation, $d_{111NaCl}^{101formamide}$ = 3.239 Å.

v$_{(111)}$ - In order to exclude the effect of the compositional sector zoning imposed by the evaporation mechanism, a complete sequence of growth experiments carried out at constant volume (from 0% to 100% formamide composition of the solvent) was performed. The saturation temperature was 95°C. Starting solutions were cooled down to −10°C with a gradient of 5 °C/hour. The 111_{NaCl} peak is unique for crystals grown from runs carried out in pure solvent (either 100% water, as in Fig.3e or 100% formamide, as in Fig. 3g), but, from all intermediate compositions of the solvent the peak shows satellite reflections, as in Fig.3f.

4.1.2. The second (2θ) interval

The behavior of the 002_{NaCl} reflection is rather different with respect to the preceding one. In this 2θ interval there is no risk of overlapping between the 002_{NaCl} peak and formamide reflections. Nevertheless, both the d_{002}^{NaCl} value and the corresponding peak profile are affected by the formamide layers absorbed in the crystal within the {111} growth sectors. In the following we will illustrate the behavior of the 002_{NaCl} peak, as for the just described situations (i-iv $_{(111)}$).

$i_{(002)}$ - C_f =20%; T_c = –5°C; T_{meas} = –5°C, as in $i_{(111)}$. A large peak is obtained, its complex profile being composed by two different contributions (Fig.3a, right side): a low angle component due to d_{002}^{NaCl} =2.814 Å and a high angle component at d_{002}^{NaCl} =2.798 Å. The averaged value of these spacing locates at d_{002}^{NaCl} averaged = 2.806 Å, which is 0.55% lower than the corresponding value calculated from the reflection d_{111}^{NaCl} = 3.258 Å observed in $i_{(111)}$. This is not surprising, if one remembers that the {111} platy shape of the crystals obtained in this case favors the dispersion of the d_{002}^{NaCl} spacing owing to the varying amount of formamide captured within the d_{111}^{NaCl} layers in the +95°C → –5°C growth interval.

$ii_{(002)}$ - C_f =20%; T_c = 30°C, by evaporation; T_{meas} = 25°C . The 002 peak profile is asymmetric (Fig.3b, right side): from the lower angle component the value ($\lambda_{K\alpha 1}$) results to be $d_{001\ lower\ angle}$ = 5.651 Å which only differs by 0.018% from the calculated d_{001} = 5.650 Å obtained from the measured d_{111} =3.262 Å, as it can be seen in $ii_{(111)}$. Further, the averaged value of the higher angle component of the asymmetric peak is located at $<d_{001}>_{higher\ angle}$ = 5.628 Å, so showing that within the same crystal population there are two generations of $<d_{001}>$ equidistances, which are differently affected by the capture of d_{101} ordered layers of formamide. In this case, the split of $<d_{001}>$ = ($<d_{001}>_{lower\ angle}$ − $<d_{001}>_{higher\ angle}$) is 0.0231Å

$iii_{(002)}$ - C_f =60%; T_c = 30°C, by evaporation; T_{meas} = 25°C . The 002 peak profile remains asymmetric, but its shape changes, due to the displacement of its two components (Fig.3c, right side). From measurement: $<d_{001}>_{lower\ angle}$ = 5.658 Å while $<d_{001}>_{higher\ angle}$ = 5.628 Å. As a consequence, the split reaches 0.0295 Å .The variation in the splitting of the two components of the 002_{NaCl} peak confirms that the increase of the formamide concentration in solution enhances as well the relative importance of the {111} surfaces and, ultimately, of the {111} growth sectors which are affected by the presence of absorbed layers of formamide. This, in turn, influences the value of the $<d_{001}>$ equidistance, according to relative portion of the {111} growth sectors which are intersected by the 001 lattice planes.

iv$_{(002)}$ - C_f =100%; T_c = 30°C, by evaporation; T_{meas} = 25°C. As for the 111 peak, the shape of the 002 reflection, located at <d_{001}> = 5.624 Å becomes symmetric (Fig.3d, right side). Compared with the corresponding <d_{001}> = 5.611 Å value, calculated from the measured 111 peak obtained under the same growth condition (see iv$_{111}$), its deviation does not exceed –0.26%.

v$_{(002)}$ - C_f ranging from 0% to 100; T_s= 95°C; T_c = –10°C; cooling rate of 5 °C/hour; T_{meas} = 25°C. 002_{NaCl} peaks resulting from all solvent compositions show satellite reflections. Starting from the decomposed XRPD data, the cell parameters calculated for each crystal cell belonging to the same growth run (same solvent composition) show a dispersion with a maximum corresponding to a C_f value close to 50% (Fig. 5).

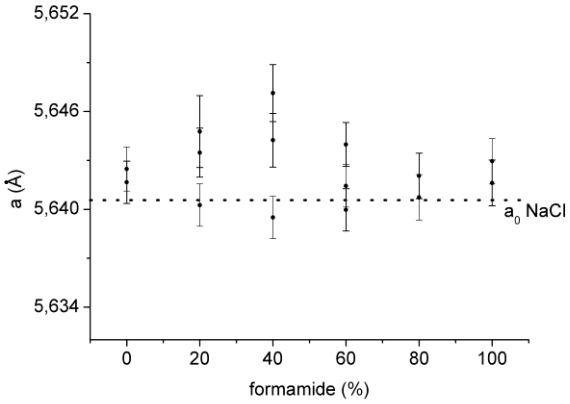

Figure 5. Cell parameter dispersion calculated from the decomposed XRPD data (referred to Fig. 3e-g).

4.2. The 2D epitaxy {101}$_{formamide}$ / {111}$_{NaCl}$ viewed through the calculation of the adhesion energy

To strengthen our initial hypothesis on the formation of 2D epitaxial layers of formamide adsorbed on the {111} form of NaCl crystal (see section 3) , we went beyond the pure geometrical constraints of the epitaxy and attempted at evaluating the interaction energy between a 2D cluster of formamide molecules and a semi-infinite underlying NaCl crystal. The 2D cluster is made by a single d_{101} layer of formamide and the NaCl surface is made by a reconstructed (and hence non polar) (111) face. Going into detail, the outmost (111) plane has a coverage degree of 25% of positive (negative) charges, while the underlying one has a coverage degree of 75% of negative (positive) charges and a third last layer recovers the

structure of the crystal bulk. This reconstruction not only cancel the intrinsic polarity of the ideal {111} form of the NaCl like crystal lattices, but respects the threefold symmetry of the face as well [26, 27].

Modeling of the $(111)_{NaCl}/(101)_{formamide}$ interface has been performed by means of atom–atom potential calculations based on OPLS-AA force field[28] as distributed with the molecular modelling package Tinker 4.2[29 a-c]. A single d_{101} formamide layer[25] comprising 50 molecules was made to interact with a $(111)_{NaCl}$ surface. A non polar reconstructed Cl^- or Na^+-terminated surface was employed with a total of 9248 NaCl units distributed over 10 NaCl layers providing an approximate size of 120 x 120 x 30 $Å^3$ for the NaCl crystal. The choice of overlayer and substrate slab size has been made based on previous successful results obtained on organic-organic hetero-epitaxial systems[30]. Simulation of the $(111)_{NaCl}/(101)_{formamide}$ interface was performed by means of docking runs with a rigid overlayer formamide crystallite free to move and interact with a rigid $(111)_{NaCl}$ surface. AutoDock3 package[31] performing Lamarckian genetic algorithm docking permitted to efficiently explore the configuration space over possible epitaxial azimuth orientations. The simulation box comprised 351^3 grid points with a sampling grid of 0.217 Å for mapping the interaction potential between substrate and overlayer. A total of 866 and 1462 docking runs were performed for the Cl^- and Na^+ terminated surface, respectively, providing a satisfactory sampling statistics of the in-plane orientations of the formamide overlayer.

The results for the Na^+ terminated $(111)_{NaCl}$ surface are reported in Figure 6a, in terms of adhesion energy averaged over the 50 formamide molecules forming the 2D cluster interacting with the substrate. First of all, it is easily seen that the adhesion energy is strongly dependent on the azimuthal orientation of the $(101)_{formamide}$ cluster with respect to the $(111)_{NaCl}$ substrate. Only few favorable azimuthal orientations were found by exploring the whole configuration space; orientations corresponding to significant adhesion energy minima were found only at $\theta = 0$ and 60° (azimuth angle θ is defined as the angle between directions $[010]_{formamide}$ and $[2\bar{1}\bar{1}]_{NaCl}$) plus their threefold symmetry equivalent orientations. The absolute minimum is found at $\theta = 0°$ (Figure 6b) and corresponds to an average

adhesion energy of ca. – 9.2 kJ/mol per molecule in the formamide cluster. The next and only significant minimum exhibits an adhesion energy about 0.6 kJ/mol higher with respect to the absolute one.

According to Boltzmann's principle, the lower energy azimuthal orientation $\theta = 0°$ is the only accessible and populated one at T close to room temperature. In fact, having assumed that critical nuclei are formed on the surface by diffusion and collisions of molecules, the lower energy azimuthal orientation at $\theta = 0°$ is preferentially selected, while the less stable orientation 0.6 kJ/mol higher shows a negligible population ratio, e.g. of 7.9×10^{-3} for only 20 formamide molecules in the nuclei.

Simulations of the Cl^- terminated $(111)_{NaCl}$ surface resulted in an absolute minimum at $\theta = 60°$ with –6.2 kJ/mol average adhesion energy per molecule while other minima cluster around $\theta = 0°$ with –5.1 kJ/mol adhesion energy (see Figure S1 in the Supporting Information). Thus, in the case of Cl^- terminated $(111)_{NaCl}$, the only significant minimum with a favorable azimuthal orientation lies at $\theta = 60°$. Compared to this result the Na^+ terminated surface therefore shows a much better adhesion energy suggesting that the (111) surface of NaCl grown in the presence of formamide could be terminated by Na^+ ions. The same proposal was put forward by Radenović et al. based on the analysis of the atomic charges for the formamide molecule[19] and by means of a SXRD study[21].

Therefore, our simulations confirm the possibility of observing 2D epitaxy between the $(111)_{NaCl}$ surface and a $(101)_{formamide}$ monolayer, strongly supporting the present interpretation of growth features of NaCl crystals in the presence of formamide.

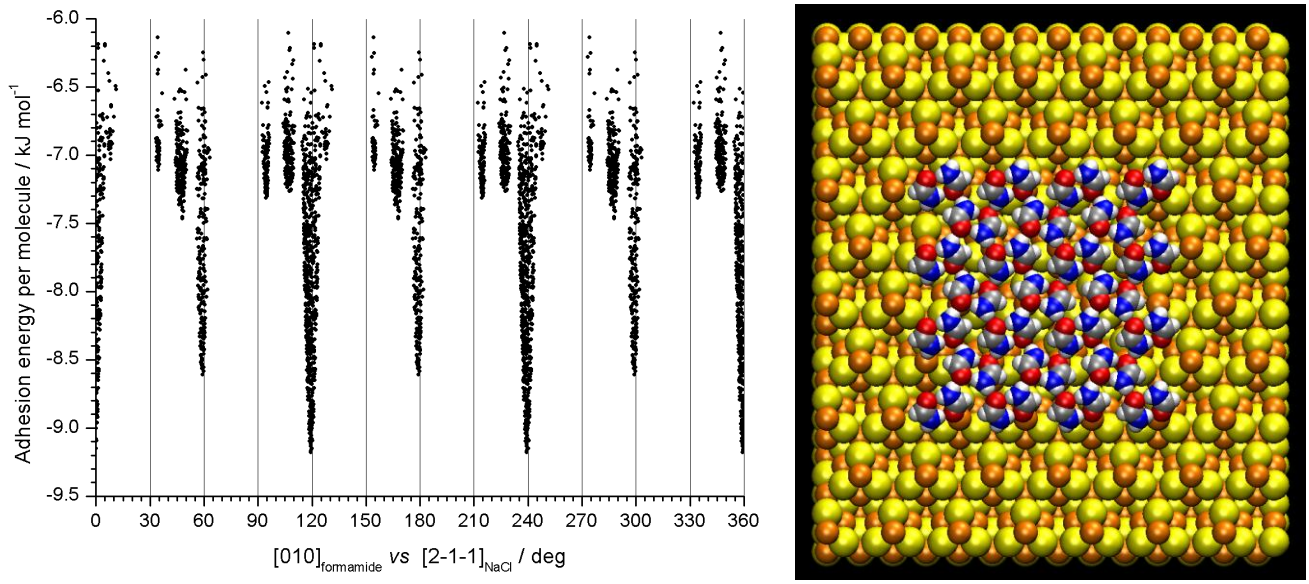

a) b)

Figure 6. (a) Summary of empirical force field calculations for a Na^+ terminated $(111)_{NaCl}$ surface showing the adhesion energy, normalized to a single formamide molecule, of the 2D cluster corresponding to a formamide d_{101} layer. (b) Sketch of a configuration corresponding to $\theta \sim 0°$ ($\theta = [010]_{formamide}$ *vs* $[2\bar{1}\bar{1}]_{NaCl}$). Atom color coding: hydrogen white, carbon silver, oxygen red, nitrogen blue, sodium orange, chlorine yellow.

5. Discussing the water/formamide competition during the adsorption onto the {111} NaCl surfaces.

It seems reasonable to hypothesize that not only formamide can be orderly adsorbed on the $\{111\}_{NaCl}$ form, but also water. As a matter of fact, a very good agreement can be found between the 2D lattice of the $\{111\}_{NaCl}$ form and that of the {0001} form of the hexagonal ice phase, the parametric misfit ($|[110]|_{NaCl} - |[210]|_{Ice}$) being lower than 2.2%. Hence, one can suppose that the $\{111\}_{NaCl}$ surfaces could act as a template for a temporary short range ordering of water at temperature higher than that of the melting point. Therefore, we can argue that the competition between water and formamide is not

only exerted in the solution bulk (solubility effect) but also at the interface level with the NaCl crystal which selectively offers its {111} surfaces as a template for the adsorption of both formamide and water.

The strong difference between the adsorbed layers of formamide and those of water (with the ice structure) lies in their thickness. In fact, the misfit (percent) between the adsorbed d_{101} layers of formamide and the d_{111} NaCl layers is – 4.769 while between the theoretically adsorbed d_{0002} layers of ice and the d_{111} NaCl layers reaches + 13.1 %. This should reasonably explain why the d_{101} formamide layers can be buried and absorbed into the NaCl crystal lattice, while the thicker d_{0002} layers of water can be only temporary adsorbed.

The hypothesis about the water orderly adsorbed on the $\{111\}_{NaCl}$ surfaces agrees as well with the growth mechanism that drives to the appearance of the $\{111\}_{NaCl}$ form when growing in pure water and in a well defined supersaturation range, as we showed in a recent work[32].

6. Conclusions

Summing up, from the detailed PXRD spectra and the calculated adhesion energy of 2D formamide layers adsorbed on the NaCl octahedron, and having considered the related changes of the overall NaCl growth morphology, one can say:

a. Formamide easily adsorbs on the $\{111\}_{NaCl}$ surfaces, so generating the morphological transition: $\{100\} \rightarrow \{100\} + \{111\}$. This change was attributed to the adsorption of isolated formamide molecules on the {111} surfaces [10, 33]. Through the observation of macrosteps spreading on the {111} surfaces (Figure1c) we found that formamide induces a K → F change in the character of the {111} form and, having found significant lattice coincidences, we put forward the hypothesis of a 2D epitaxy setting up between the $101_{formamide}$ lattice planes and the $\{111\}_{NaCl}$ surfaces. Calculation of the adhesion energy of 2D formamide (101) layers adsorbed on the {111} NaCl form allows to state that the most reasonable model of formamide adsorption is not "random-molecular" but "2D-epitaxial islands", even if the growth solution is unsaturated with respect to formamide.

b. The thickness of the epitaxially adsorbed $d_{101}^{formamide}$ layers fits very well ($\Delta d<5\%$) with the height of the elementary d_{111} steps of NaCl crystals. Hence, one can reasonably suppose that the ordered adsorbed layers can be easily buried in the $\{111\}_{NaCl}$ sectors during growth.

c. PXRD diagrams carried out on as-grown NaCl crystal populations, under different temperature of crystallization (T_c) and formamide concentration (C_f) in aqueous solutions, showed that the 111 and 002 reflections of NaCl are profoundly and differently modified according to both T_c and C_f values, the main factor of change being the relative size of the "formamide contaminated $\{111\}_{NaCl}$ growth sectors". This unambiguously proves our hypothesis put forward in (b).

d. When NaCl crystals nucleate and grow from pure formamide solution, PXRD diagrams indicate that only the {111} growth sectors exist in the crystals.

e. Cell parameters, as obtained from the decomposition of the PXRD diagrams, show the highest dispersion when the ratio between the concentration of the two solvents (water/formamide) is approximately 1. This effect could be related to the competition between the solvents during the adsorption onto the octahedral surfaces of the halite crystal.

Finally, we can conclude that "anomalous NaCl/formamide mixed crystals" form in the {111} growth sectors only, at T >2°C and at different C_f values in aqueous solutions. However, when C_f =100%, then the "anomalous NaCl/formamide mixed crystals" occupies all the crystal volume, simulating the behavior of a "homogeneous" crystal. This means that we have not to do, of course, with a solid solution but with NaCl crystals in which clusters of formamide layers are uniformly distributed in the growing crystals.

Acknowledgements

We thank prof. Raymond Kern (CINAM- Marseille), prof. Marco Rubbo and Dr. Roberto Cossio (DST- Torino University) for many fruitful discussions and suggestions and Dr. Angelo Agostino (Chemistry Department - Torino University) for PXRD measurements.

Supporting Information Available

111 NaCl peak **002 NaCl peak**

a)

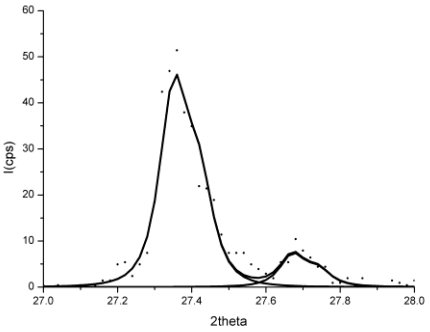

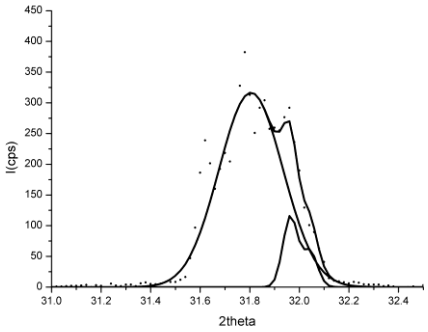

b)

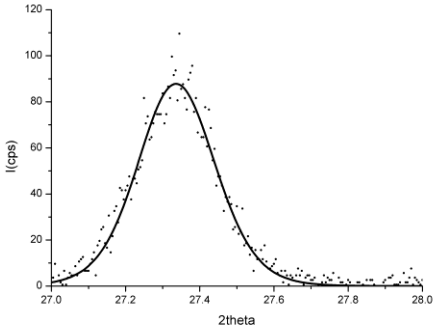

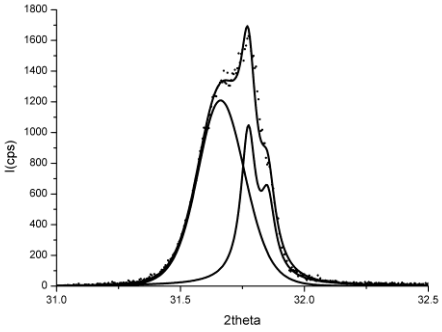

c)

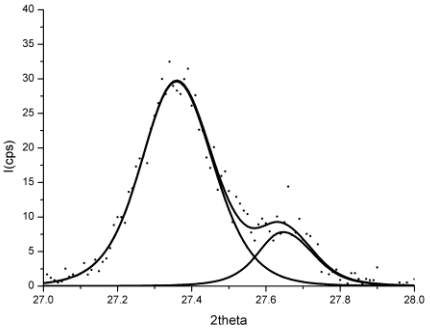

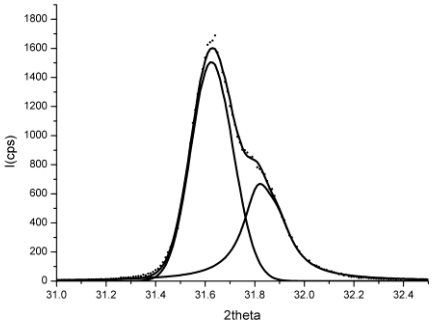

111 NaCl peak **002 NaCl peak**

d)

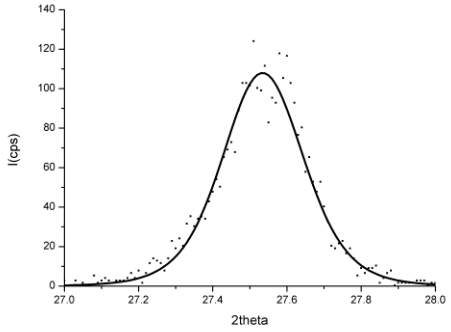

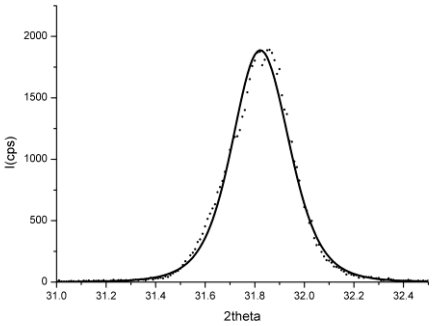

e)

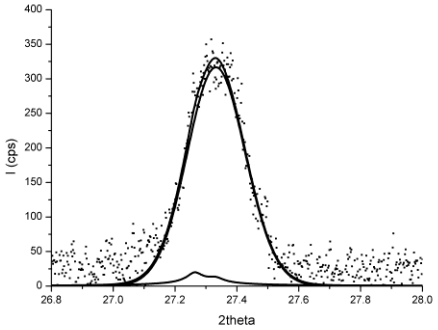

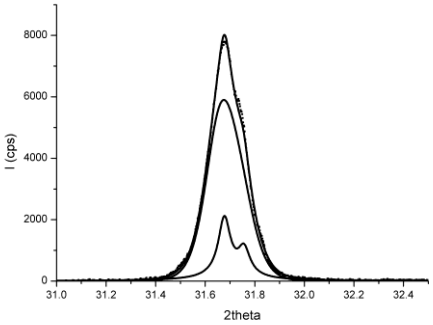

f)

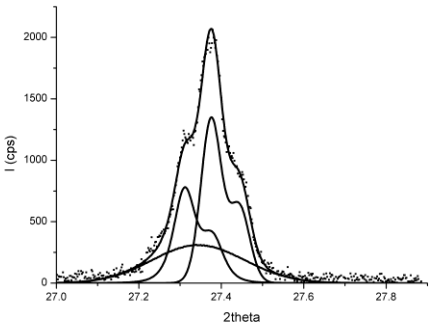

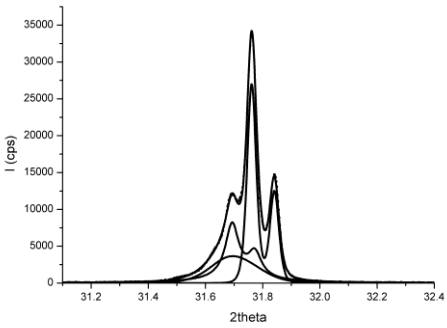

g)

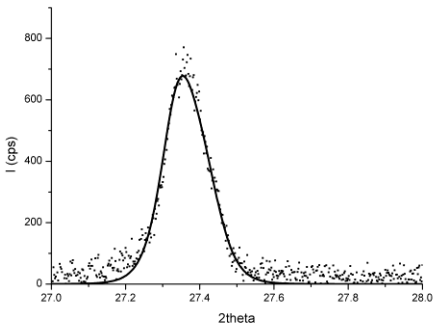

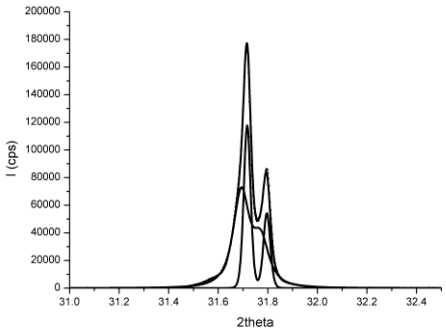

Figure S1. Diffraction data were fitted using a symmetric Pearson VII distribution considering both Cu $\lambda_{K\alpha1}$ and $\lambda_{K\alpha2}$ radiations with a refined $\lambda_{K\alpha1/K\alpha2}$ ratio of 0.48.

Reflection	**°(2θ)**	**a**	**b**	**c**	**d**	**e**	**f**	**g**
		from evaporation				*from cooling*		
							27.201	
						27.264		
							27.292	
			27.315			27.313		
				27.340				27.343
		27.351						
d_{111} NaCl	27.360							
							27.384	
					27.513			
				27.631				
		27.671						
d_{101} formamide	28.823							
							31.552	
				31.603				
			31.640					
						31.66		
						31.677	31.673	
								31.693
d_{002} NaCl	31.700							
							31.718	31.717
		31.779	31.773					
					31.798			
				31.812				

		31.964						

Table S2. Peak position distribution of d_{111} NaCl, d_{101} Formamide and d_{002} NaCl (Cu $\lambda_{K\alpha 1}$ only) with respect to the compositional changes of the solution as obtained from the PXRD decomposition in Figure S1.

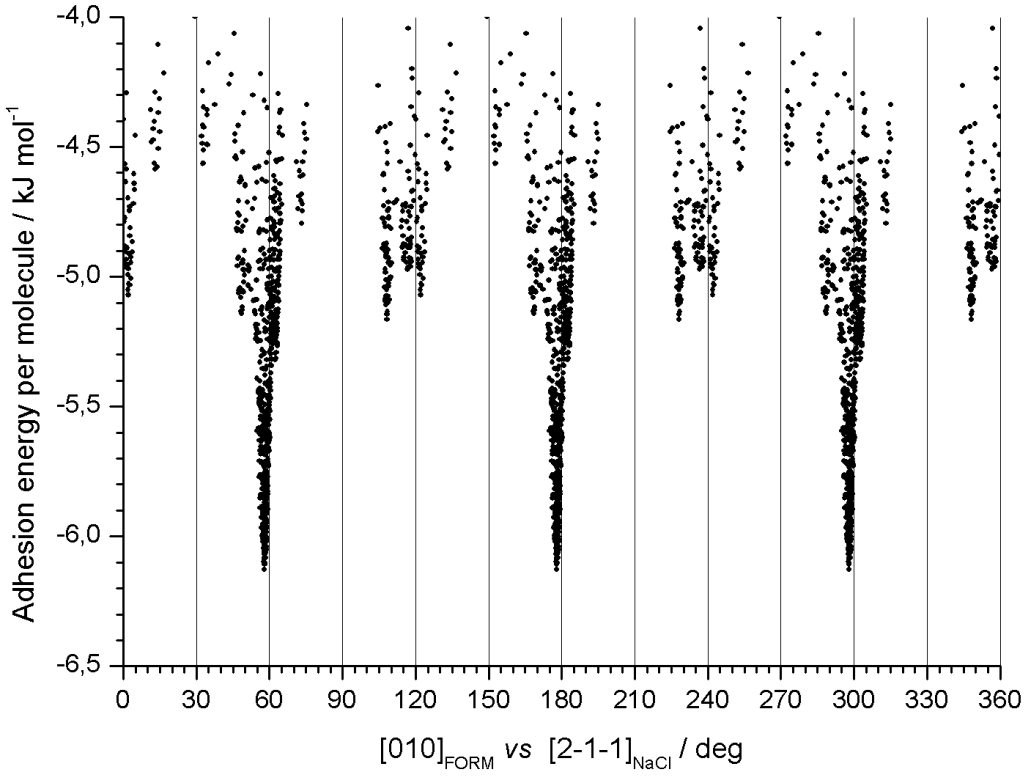

Figure S3. Summary of empirical force field calculations for a Cl^- terminated (111) NaCl surface showing the adhesion energy, normalized to a single formamide molecule, of the 2D cluster comprising a formamide d_{101} layer.

References

(1) a) Pastero, L. ; Costa, E. ; Bruno, M. ; Rubbo, M.; Sgualdino, G. ; Aquilano, D. *Cryst. Growth Des.* **2004,** *4(3)*, 485-490; b) Pastero, L. ; Aquilano, D. ; Costa, E. ; Rubbo, M. *J. Cryst. Growth* **2005,** *275*, e1625- e1630; c) Massaro, F.R. ; Pastero, L. ; Costa, E. ; Sgualdino, G. ; Aquilano, D. *Cryst. Growth Des.* **2008**, *8(6)*, 2041-2046.

(2) Gaubert, P. *Bull. Soc. fr. Minéral.* **1900**, *23*, 211; **1905**, *28*, 180; *Publ. Soc. Chimie Physique*, Hermann, Paris **1915**, *38*, 149; **1902**, *25*, 242; *Comptes rendus* **1918**, *167*, 491; **1925**, *180*, 378 .

(3) Seifert, H. *Fortschritte Miner*. a) **1935**, *19*, 103; b) **1936**, *20*, 324; c) **1937**, *22*, 185.

(4) Johnsen, A. *Neues Jahrb. Miner*. Bd.II **1903**, *93*

(5) Neuhaus A. *Chemie der Erde* a) **1930**, *5*, 529 ; b) **1930**, *5*, 544; *Zeit. Krist*. a) **1937**, *97*, 28 ; b) **1937**, *97*, 112; c) **1941**, *103*, 297 ; d) **1942,** *104*, 197; e) **1944**, *105*, 161.

(6) Hartman, P. in *Adsorption et Croissance Cristalline,* Colloques Internat. du CNRS n°152 (CNRS-Paris) **1965**, 477-513.

(7) Pastero, L. ; Aquilano, D. *Cryst. Growth Des*. **2008**, *8 (9),* 3451–3460.

(8) Aquilano, D.; Bruno, M. ; Massaro, F.R. ; Rubbo,M. *Cryst. Growth Des*. **2011**, *11,* 3985-3993.

(9) Gille, F.; Spangenberg, K. Z. Kris. Miner. Petrograd. 1927, A65, 204

(10) Bienfait, M.; Boistelle, R.; Kern, R. in Adsorption et Croissance Cristalline , Colloques Internat. du CNRS n°152 (CNRS-Paris) 1965, 577 – 592

(11) Romé de l'Isle, J.B.L. *Cristallographie* (2nd ed., 4 v., Paris, Imprimerie de Monsieur, 1783) .

(12) a) Chernov, A.A. Modern Crystallography III: Crystal Growth, Springer, Berlin, 1984. b) Sangwal, K. *J. Crystal Growth* **1993**, *128*, 1236-1244 c) Sangwal, K. *Prog. Crystal Growth Charact.*

1998, *38*, 163 d) Furedi-Milhofer, H.; Sarig, S. *Prog. Crystal Growth Charact.***1996**, *32*, 45-74 e) Veintemillas-Verdaguer, S. *Prog. Crystal Growth Charact.* **1996** , *32*, 75-109

(13) a) Boistelle, R.; Kern, R.; Weiss, R. *C. R. Acad. Sci.* **1962**, *254*, 1829 b) Bienfait, M.; Boistelle, R.; Kern, R. *C. R. Acad. Sci.* **1963**, *256*, 2189. c) Roland, C.T.; Ralston, P.H. Canadian Patent No. 765.644, **1963**. d) van Damme-van Weele, I.M.A. *Influence of additives on the Growth and Dissolution of Sodium Chloride Crystals*, PhD. Thesis, Techn. Univ. Twente, Enschede, (NL), **1965**; van Damme-van Weele, I.M.A. in: R. Kern (Ed.), *Adsorption et Croissance Cristalline*, Coll. CNRS **1965**, *152*, 433 e) Glasner, A.; Zidon, M. *J. Crystal Growth* 21 (1974) 294 - 304 f) H.H. Emons, H.H. Freiberg. Forschungsh. A 600 (1979) 73.

(14) a) Selwitz, C.; Doehne, E. *J. Cultural Heritage* **2002,** *3*, 205-216 b) Rodriguez-Navarro, C.; Linares-Fernandez, E.; Doehne, E.; Sebastian, E. *J. Cryst. Growth* **2002**, *243*, 503– 516

(15) a) Transportation Research Board, Special Report 235, Highway De-icing: Comparing Salt and Calcium Magnesium Acetate, National Research Council, Washington, DC, 1991. b) Salt Institute, De-icing Salt and Our Environment. Salt Institute, Alexandria VA, 1996.

(16) Hansen, T.B.; Skibsted, L.H.; Andersen, H.J. *Meat Sci.* **1996**, *43*, 135 - 144

(17) Bienfait, M.; Kern, R.; Mutaftschiev, B. *Z. Krist.* **1964**, *120*, 466

(18) Radenović, N.; van Enckevort, W.J. P. *J. Cryst. Growth* **2002**, *234*, 589 –598

(19) Radenović, N.; van Enckevort, W.J. P. ; Verwer, P.; Vlieg, E. *Surf. Sci*. **2003**, *523*, 307-315.

(20) Radenović, N.; van Enckevort, W.J. P.; Vlieg, E. *J. Cryst. Growth* **2004**, *263*, 544 –551

(21) Radenović, N.; Kaminski, D.; van Enckevort, W.J. P. ; Graswinckel, S.; Shah, I.; in ‘t Veld, M.; Algra, R.; Vlieg, E. *J. Chem. Phys*. **2006**, *124*, 164706-164712.

(22) Radenović, N. *The role of impurities on the morphology of NaCl crystals – An atomic scale view*, PhD Thesis, **2006**, Radboud University, Nijmegen (NL).

(23) Ladell, J.; Post, B. *Acta Cryst*. **1954**, *7*, 559- 564.

(24) Ottersen, T. *Acta Chem.Scand*. **1975**, *A 29*, 939-944.

(25) Stevens, E.D. *Acta Cryst*. **1978**, *B34*, 544-551.

(26) Bruno, M.; Aquilano, D.; Pastero, L.; Prencipe, M. *Cryst. Growth Des.* **2008**, *8 (7),* 2163-2170.

(27) Bruno, M.; Aquilano, D.; Prencipe, M. *Cryst. Growth Des.* **2009,** *9(4)*, 1912-1916

(28) Jorgensen, W. L.; Maxwell, D. S.; Tirado-Rives, J. *J. Am. Chem. Soc.* **1996**, *118*, 11225-11236

(29) a) Ponder, J.W. *TINKER: Software Tools for Molecular Design, Version 4.2.* **2004**, Washington Univ. School Medicine: Saint Louis, MO, 2003. b) Ren, P.; Ponder, J. W. *J. Comput. Chem*. **2002**, *23*, 1497-1506. c) Ren, P.; Ponder, J. W. *J. Phys. Chem.* **2003**, *B 107*, 5933-5947

(30) a) Haber, T.; Resel, R.; Thierry, A.; Campione, M.; Sassella, A.; Moret, M. *Physica* **2008**, *E 41*, 133-137; b) Campione, M.; Moret, M.; Raimondo, L.; Sassella,A. *J. Phys. Chem*. **2009**, *C 113*, 20927-20933; c) Campione, M.; Raimondo, L.; Moret, M.; Campiglio,P.; Fumagalli, E.; Sassella, A. Chem. Mater. **2009**, *21*, 4859-4867; d) Raimondo, L.; Moret, M.; Campione, M.; Borghesi, A.; Sassella, A. *J. Phys. Chem.* **2011**, *C 115*, 5880-5885; (e) Moret, M.; Borghesi, A.; Campione, M.; Fumagalli, E.; Raimondo, L.; Sassella, A. *Cryst. Res. Technol.* **2011**, *46*, 827-832.

(31) Morris, G.M.; Goodsell, D.S.; Halliday, R.S.; Huey, R.; Hart,W.E.; Belew,R.K.; Olson, A.J. *J. Comput. Chem.* **1998***, 19*, 1639-1662

(32) Aquilano, D.; Pastero, L.; Bruno, M.; Rubbo, M. J. Cryst. Growth **2009**, *311*, 399-403.

(33) Singh, A.; Kesharwani, M.K.; Ganguly, B. *Cryst. Growth Des*. **2009**, *9*, 77 - 81

TOC

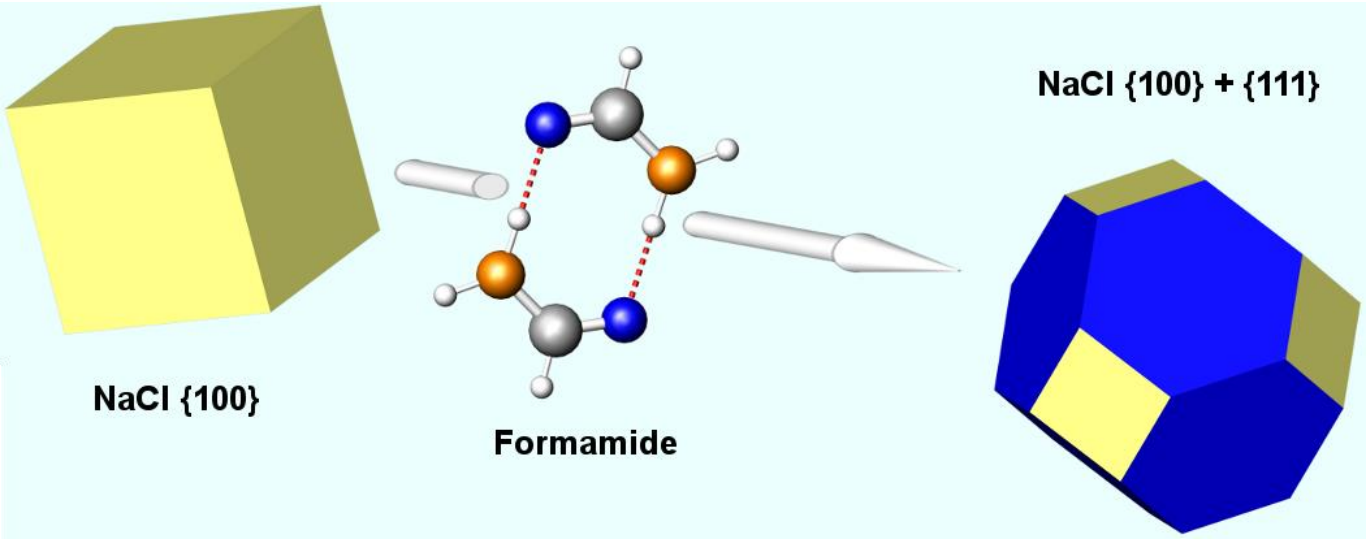

Synopsis

The crystal morphology of NaCl crystals changes from {100} (pure aqueous solution) to {100} + {111} (water-formamide solutions) to {111} (pure formamide solution). PXRD diagrams prove that formamide is epitaxially adsorbed on the {111} NaCl and then is selectively captured within the {111} growth sectors, due to the striking equivalence between the thickness of the elementary layers d_{111}^{NaCl} and $d_{101}^{formamide}$. Hence, formamide is not only an habit modifier of NaCl crystals, since "anomalous NaCl / formamide mixed crystals" form, limited to the {111} NaCl growth sectors.

For Table of Contents Use Only

Selective adsorption / absorption of formamide in NaCl crystals growing from solution

Linda Pastero[1]*, Dino Aquilano[1] and Massimo Moret[2]

[1]*Dipartimento di Scienze della Terra, Università degli Studi di Torino – Via Valperga Caluso 35 I-10125 Torino*

[2]*Dipartimento di Scienza dei Materiali, Università degli Studi di Milano Bicocca - Via Roberto Cozzi 53 – I- 20125 Milano*